Journal of Applied Polymer Science

# Hyperbranched polyglycerol/poly(acrylic acid) hydrogel for the efficient removal of methyl violet from aqueous solutions

**Hao Ying, Guijin He, Lifeng Zhang, Qunfang Lei, Yongsheng Guo, Wenjun Fang**

Department of Chemistry, Zhejiang University, 38 Zheda Road, Hangzhou 310027, People's Republic of China

The authors of this article contributed in the following ways. H. Ying and W. Fang designed the research and wrote the article. H. Ying, G. He, and L. Zhang performed the research and analyzed the data. Q. Lei, Y. Guo, and W. Fang polished the article.

Correspondence to: W. J. Fang (E-mail: fwjun@zju.edu.cn)

**ABSTRACT:** Hydrogels were synthesized from hyperbranched polyglycerol (HPG) and acrylic acid through free-radical polymerization with HPG as the crosslinker. The HPG/poly(acrylic acid) (PAA) hydrogel could absorb cationic dyes in aqueous solutions because of the existence of a porous structure and the large numbers of hydroxyl and carboxylic groups. With methyl violet chosen as a model compound, the HPG/PAA hydrogel reached a maximum adsorption of 394.12 mg/g at a feed concentration of 1 g/L. The highest removal ratio of 98.33% was observed at a feed concentration of 50 mg/L. The effects of the pH, contact time, and feed concentration on the dye adsorption were investigated. The dye adsorption data fit well with the pseudo-second-order and Langmuir models. We believe that the HPG/PAA hydrogels could perform well in appropriate applications in the removal of cationic dyes from aqueous solutions because of their high adsorption capacity and environmental friendliness. © 2015 Wiley Periodicals, Inc. J. Appl. Polym. Sci. **2016**, *133*, 42951.

**KEYWORDS:** adsorption; crosslinking; hydrophilic polymers

Received 19 May 2015; accepted 16 September 2015

**DOI: 10.1002/app.42951**

## INTRODUCTION

Chemical industries, such as textiles, plastics, and printing, use more than 10,000 different dyes for coloring their products.[1] However, the effluents discharged by factories may cause serious environmental pollution.[2–4] Dye removal from contaminated water is considered a worldwide problem and has drawn attention from academia and industry. Treatments of membranes,[5,6] coagulation/flocculation,[7] ion exchange,[8] and biodegradation[9,10] have quickly been developed to solve this problem.

In 1982, Maciejewski[11] analyzed the structure of dendritic polymers and indicated the possibility of their capturing small molecules within a dense shell of peripheral groups. Since then, the applications of dendritic polymers in host–guest chemistry have been developed.[12,13] As a typical dendritic polymer, hyperbranched polyglycerol (HPG) possesses highly flexible aliphatic polyether backbones, multiple hydrophilic groups, and excellent biocompatibility. It has been widely used in science, medicine, and engineering.[14–18] The properties of HPG can be regulated or altered to produce various functional architectures. Recently, Burakowska and his coworkers[19,20] synthesized crosslinked HPG through a ring-closing metathesis reaction and successfully developed its application for dye adsorption and release. Zhou *et al.*[21] developed a magnetic dendritic material with oxide-silica particles and carboxylic HPG. This material was further applied to dye removal, and it showed a good dye adsorption capacity.

In this study, to prepare an absorbent with large amounts of hydrophilic groups and the advantages of easy preparation, nontoxicity, and easy separation from aqueous solutions, HPG and acrylic acid (AA) were chosen to form hydrogels for the removal of methyl violet (MV) in aqueous solution. Compared with previous studies, in this study, we explored a new exploration of HPG hydrogels in the field of dye adsorption. Therefore, it was necessary to comprehensively study the chemical composition, network structure, swelling behavior, and adsorption properties of the HPG/poly(acrylic acid) (PAA) hydrogels.

## EXPERIMENTAL

### Materials

Glycidol was purchased from Sigma-Aldrich. Glycidyl methacrylate, 4-(*N*,*N*′-dimethyl amino)pyridine, AA, 2,2-azobisisobutyronitrile (AIBN), 1,1,1-tris(hydroxymethyl)propane, and dimethyl sulfoxide were purchased from Aladdin Chemical Reagent Co. MV was purchased from Shanghai Yuanhang Reagent Co. All of the reagents were used as received without further purification.

**Table I.** Feed Compositions of the HPG/PAA Hydrogels

| | Sample | | | | |
|---|---|---|---|---|---|
| Component | HA1 | HA2 | HA3 | HA4 | HA5 |
| HPG-MA (g) | 5 | 4 | 3 | 2 | 1 |
| AA (g) | 1 | 2 | 3 | 4 | 5 |
| $H_2O$ (mL) | 20 | 20 | 20 | 20 | 20 |
| AIBN (g) | 0.06 | 0.06 | 0.06 | 0.06 | 0.06 |
| Calculated PAA amount (%) | 16.6 | 33.3 | 50.0 | 66.6 | 83.3 |
| Experimental PAA amount (%) | 19.8 | 37.2 | 54.7 | 67.4 | 85.4 |

### Preparation of the HPG and Methacrylated Hyperbranched Polyglycerol (HPG-MA)

We prepared HPG and HPG-MA with the procedures and reactants described by Sunder *et al.*[22] and Oudshoorn *et al.*[23] We partially deprotonated (10%) 1,1,1-Tris(hydroxymethyl)propane (1.68 g) with 0.2 mL of a potassium methylate solution (1.25 mmol of $CH_3OK$) by distilling off excess methanol from the melt. Glycidol (50 mL) was slowly added at 95°C over 12 h under a nitrogen atmosphere. The product was neutralized by filtration over a cation-exchange resin and precipitated twice from the methanol solution into acetone. Finally, HPG was dried at 80°C *in vacuo*. The synthesis of HPG-MA was carried out in a three-necked flask. HPG (1 g) was dissolved in dimethyl sulfoxide (9 mL) at room temperature under a nitrogen atmosphere. Next, 4-(*N*,*N*′-dimethyl amino)pyridine (2 g) and glycidyl methacrylate (2.51 mL) were added. After 5 h of stirring at room temperature, HPG-MA was precipitated in ethyl ether and dried at room temperature.

### Preparation of the HPG/PAA Hydrogels

HPG-MA, AA, and AIBN were dissolved in 20 mL of deionized water with magnetic stirring. Nitrogen was purged for 15 min to remove the dissolved oxygen in the three-necked flask. The gelation was maintained at 80°C for 2 h to obtain the HPG/PAA hydrogel. The hydrogel was then kept in ionized water for 12 h to remove unreacted AA and HPG-MA. Finally, the HPG/PAA hydrogel was dried at 80°C *in vacuo*. We prepared different hydrogels by changing the mass ratio of HPG-MA to AA. The compositions for the investigated HPG/PAA hydrogels are listed in Table I. The experimental PAA contents in the hydrogels were calculated from the thermogravimetric analysis (TGA) results, and these results are also shown in Table I.

### Characterization of the HPG/PAA Hydrogels

**Fourier Transform Infrared (FTIR) Analysis.** The HPG/PAA hydrogels were analyzed with an FTIR spectrophotometer (Nicolet 5700) with a scanning wave-number range from 4000 to 550 $cm^{-1}$. The hydrogels were freeze-dried overnight, and the dried hydrogels were ground into powder and mixed with KBr powder. The mixed samples were compressed into small slices and analyzed by the FTIR spectrophotometer.

**TGA.** TGA of the HPG/PAA hydrogels was carried out on a TA instrument (TA Q50) under a nitrogen atmosphere at a scanning rate of 10°C/min in the temperature range 20–600°C.

**Microscopic Observation.** To retain the integrity of the hydrogel network, a dry HPG/PAA hydrogel was brittlely fractured in liquid nitrogen and coated with a gold layer. Subsequently, its network structure was observed and photographed with scanning electron microscopy (SEM; Hitachi SU8000) at an accelerated voltage of 5.0 kV.

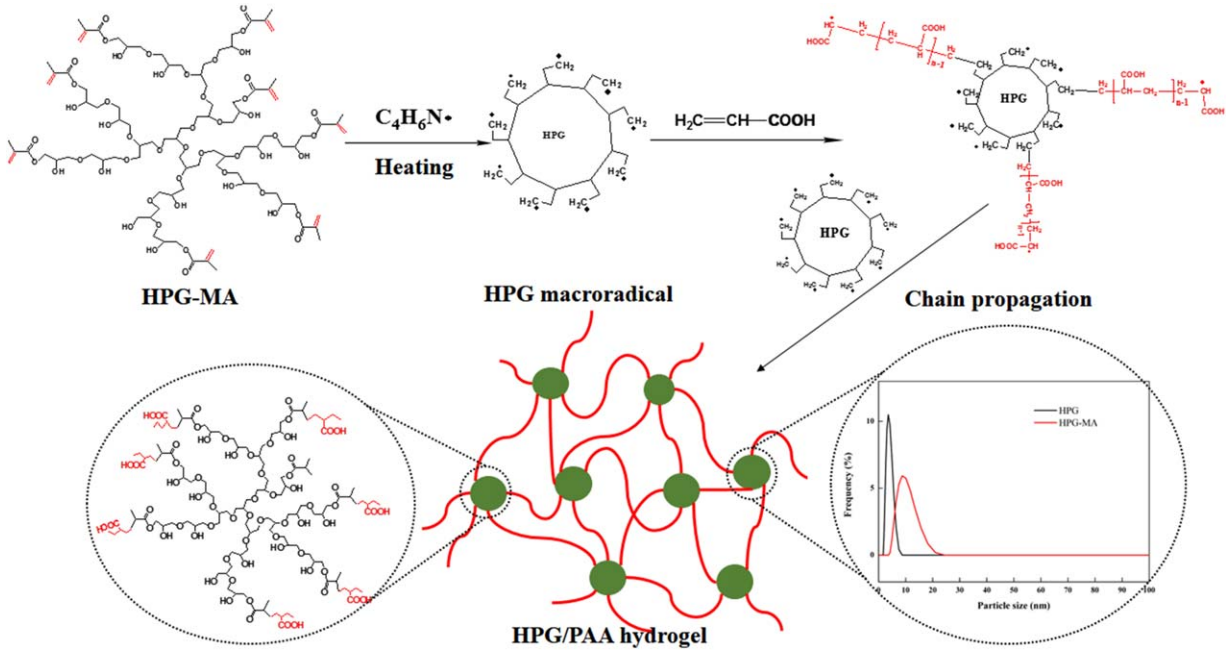


**Figure 1.** Formation mechanism of the HPG/PAA hydrogels. [Color figure can be viewed in the online issue, which is available at wileyonlinelibrary.com.]

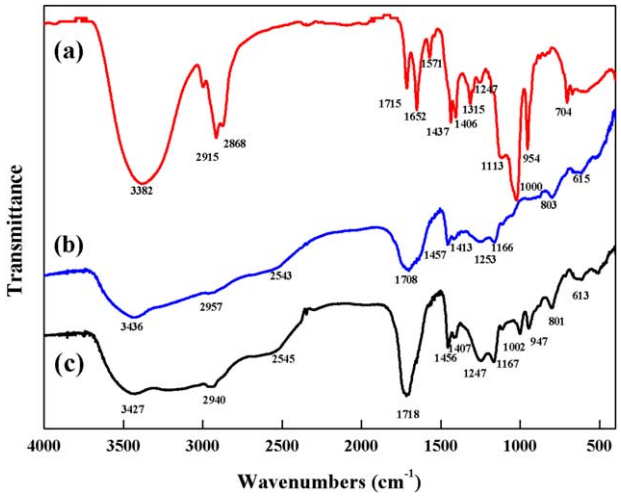


**Figure 2.** FTIR spectra of (a) HPG-MA, (b) PAA, and (c) HPG/PAA. [Color figure can be viewed in the online issue, which is available at wileyonlinelibrary.com.]

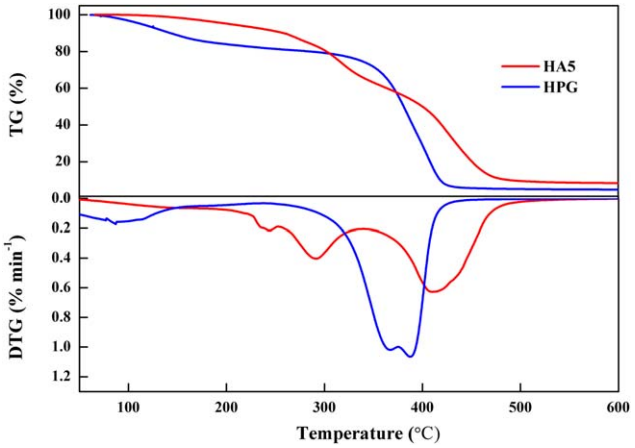


**Figure 3.** TGA results for the HPG and HPG/PAA hydrogels (TG = thermogravimetry; DTG = derivative thermogravimetry). [Color figure can be viewed in the online issue, which is available at wileyonlinelibrary.com.]

### Investigations of the Swelling Behaviors of the HPG/PAA Hydrogels

**Influence of the Temperature on the Swelling Ratio.** The influence of the temperature on the swelling ratio of the HPG/PAA hydrogels was investigated in deionized water, and the swelling ratio was looked at as a function of the temperature. The swelling ratio of the hydrogel sample was measured with a gravimetric method from 15 to 70°C at intervals of 5°C. The dry hydrogel, after measurement, was immersed in deionized water for swelling. After 24 h, the hydrogel was hung in air for 3 min to get rid of water on the surface. The swelling ratio ($S$) was calculated as follows:

$$S = \frac{W_t - W_0}{W_0} \quad (1)$$

where $W_t$ is the weight of the swollen hydrogel and $W_0$ is the weight of the dried hydrogel.

**Influence of the pH on the Swelling Ratio.** The influence of the pH on the swelling ratio of the HPG/PAA hydrogels was studied in phosphate buffer solutions at pH 1.0–13.0. The desired pH value was adjusted by HCl and NaOH solutions and was precisely checked by a pH meter (Mettler-Toledo S400). Then, the dried hydrogel was immersed in the buffer solution for swelling, and the swelling ratio was measured with the gravimetric method as well.

**Influence of Salt on the Swelling Ratio.** The influence of salt on the swelling ratio of the HPG/PAA hydrogels was studied in different salt solutions with concentrations of 0.1 mol/L. The swelling ratio was measured with the gravimetric method as well.

**Swelling Kinetics.** The dynamic swelling properties of the hydrogels were investigated in deionized water at 25°C. The swelling ratios of the HPG/PAA hydrogel at various time intervals were fitted to the following second-order rate equation:

$$S_t = \frac{S_{ecal}^2 k_2 t}{1 + k_2 S_{ecal} t} \quad (2)$$

where $S_t$ is the swelling ratio at time $t$, $S_{ecal}$ is the calculated equilibrium swelling ratio, and $k_2$ is the rate constant of the pseudo-second-order.

### Dye Removal Capacity of the Hydrogels

A weight of 50 mg of hydrogel was immersed into each of the 50-mL MV solutions with different concentrations. After the equilibrium adsorption ($q_e$; mg/g) was reached, the concentration of MV in the solution was determined from a precalibrated curve of the absorbance versus the concentration with an ultraviolet–visible spectrophotometer (Shimadzu 1240) at $\lambda_{max}$(maximum absorbance) = 582 nm. The effects of the pH (1–13), adsorption time, and feed concentration (50–550 mg/L) on the dye adsorption were investigated. We calculated the $q_e$ and removal ratio ($R$) with the following equations:

$$q_e = \frac{C_0 - C_e}{m} V \quad (3)$$

$$R = \frac{C_0 - C_e}{C_0} \times 100\% \quad (4)$$

where $C_0$ is the initial concentration of the MV solution, $C_e$ is the equilibrium concentration of the MV solution, $V$ is the volume of the MV solution, and $m$ is the mass of the dry hydrogel.

The adsorption data were fitted to pseudo-first-order, pseudo-second-order, Langmuir, and Freundlich models to investigate the kinetics and isotherms. The mass-transfer coefficient was also investigated.

## RESULTS AND DISCUSSION

### Formation Mechanism of the HPG/PAA Hydrogels

As shown in Figure 1, the HPG/PAA hydrogels were prepared with HPG and AA as monomers and AIBN as the initiator through free-radical polymerization. When the mixture was heated, 2-cyano propyl radicals were generated from the decomposition of AIBN. Then, the addition reactions between 2-cyano propyl radicals and AA molecules took place to produce the monomer radicals.[24,25] Meanwhile, the vinyl groups of HPG-

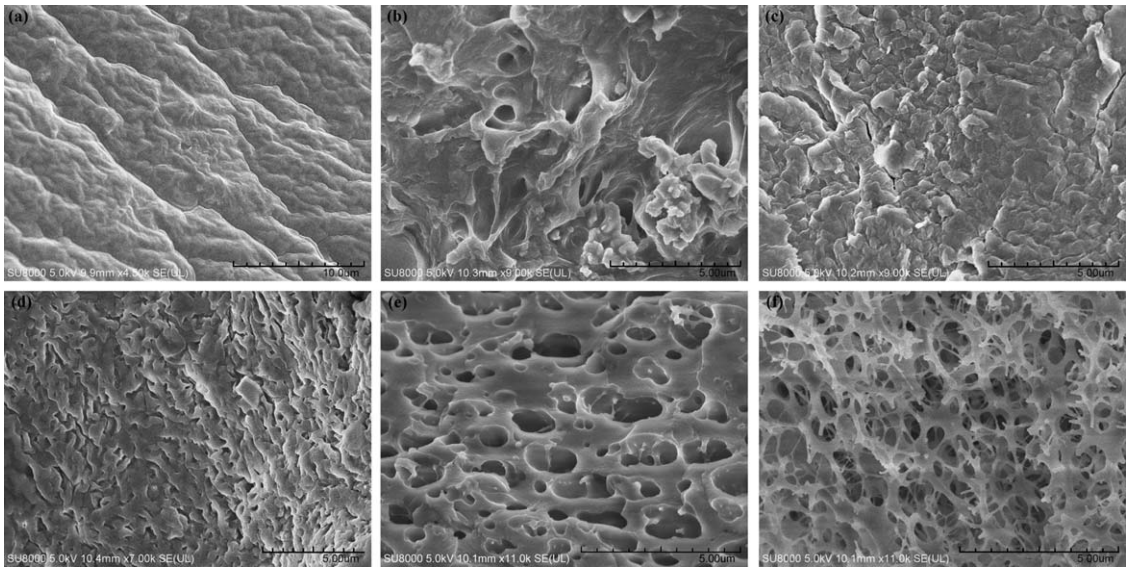


**Figure 4.** SEM images of the HPG/PAA hydrogels: (a) HPG hydrogel, (b) HA1, (c) HA2, (d) HA3, (e) HA4, and (f) HA5.

MA were activated by the 2-cyanopropyl radicals, and the HPG molecules were changed into macroradicals. These macroradicals acted as active centers during the chain propagation, and finally, the PAA chains connected to different HPG molecules to form a crosslinked network structure.[26] The dynamic light scattering result shows that the average particle sizes of HPG and HPG-MA were about 4.2 and 8.2 nm, respectively. When immersed into alkaline solutions of pH 8–13, the PAA hydrogel could decompose into liquid because of the elimination of hydrogen-bond interactions, whereas the HPG/PAA hydrogels remained stable. Therefore, we concluded that HPG acted as crosslinker, even at a small quantity because of the high relative surface area.

### Chemical Structure

The FTIR spectra of one sample (HA3) of the HPG/PAA hydrogels and HPG-MA and PAA are shown in Figure 2. For the HPG/PAA hydrogel, a strong and broad absorption band appearing at 3427 $cm^{-1}$ indicated O—H and C—OH stretching. The absorption band at 2940 $cm^{-1}$ was due to the asymmetric and symmetric stretching vibrations of the methylene group in HPG and PAA. The absorption peak at 1718 $cm^{-1}$ was ascribed to the C=O stretching in carboxyl groups. The absorption peaks at 1456 and 1407 $cm^{-1}$ were due to the $COO^-$ asymmetric stretching and symmetric stretching of carboxylate anion.[27–29] The absorption peaks at 1247 and 1167 $cm^{-1}$ were due to the C—O—C stretching of HPG. The absorption peaks at 1002 and 947 $cm^{-1}$ corresponded to the C=C—H bending vibrations.[27] It was clear that the spectrum of HPG/PAA was similar to that of PAA; this indicated the existence of PAA chains in the HPG/PAA hydrogels. Compared with HPG-MA, the absorption peak of vinyl at 1652 $cm^{-1}$ disappeared, and the absorption peaks at 1002 and 947 $cm^{-1}$ obviously weakened. This phenomenon confirmed that the PAA chains successfully connected to different HPG molecules to form a hydrogel. Overall, it illustrates the presentation of HPG and AA in the

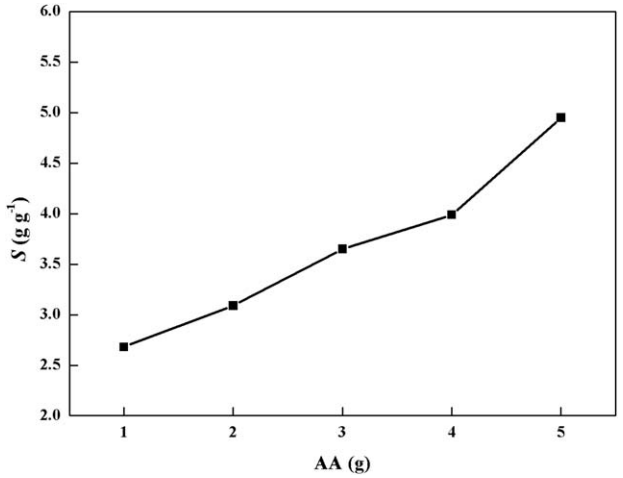


**Figure 5.** Effect of the PAA content on the swelling ratio of HPG/PAA hydrogels.

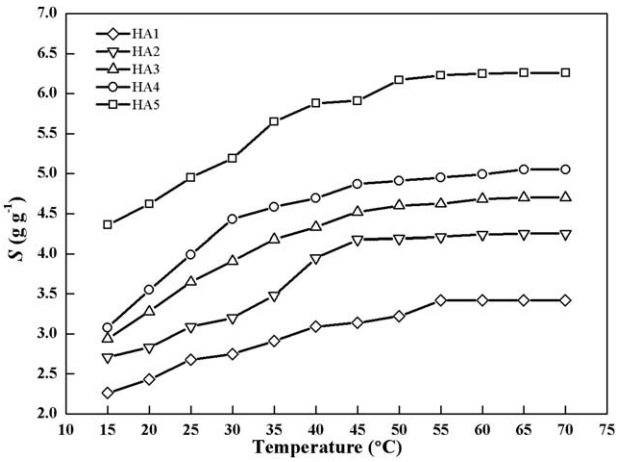


**Figure 6.** Temperature dependence of the swelling ratio of the HPG/PAA hydrogels.

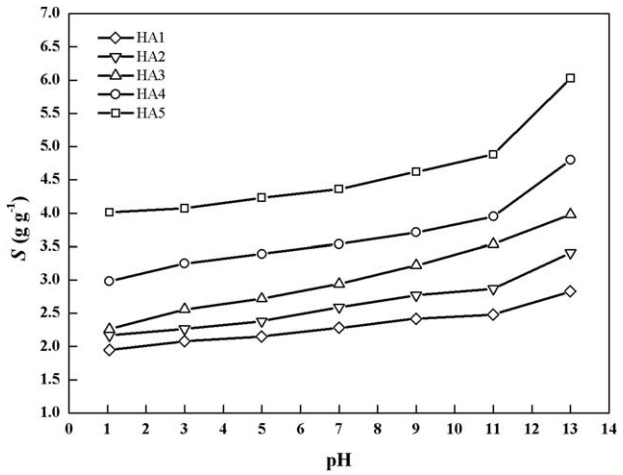


**Figure 7.** pH dependence of the swelling ratio of the HPG/PAA hydrogels.

hydrogels and verifies the validity of the previously discussed formation mechanism of the HPG/PAA hydrogels.

### Thermal Stability

The thermal decomposition of all of the HPG/PAA hydrogels was investigated by TGA, and the results were used to determine the actual content of each polymer in the hydrogels. HA5 and HPG were chosen as examples and are shown in Figure 3. It was observed that the HPG hydrogel showed a weight loss around 20 wt % up to a temperature of 200°C; this was due to the loss of absorbed water. In the temperature range 255–420°C, the HPG hydrogel underwent decomposition of its polyether skeleton with a weight loss of nearly 100%; this was similar to the decomposition of poly(ethylene glycol).[30] The HPG/PAA hydrogel showed a multiple-step degradation, which was due to the different degradation profiles of its constituents. The weight loss around 10% in the temperature region of 100–200°C was due to the loss of absorbed water. The 15–40 and 40–90 wt % weight losses in temperature regions of 200–310 and 330–500°C, respectively, were ascribed to the elimination of water molecules from the hydroxyl and carboxylic groups, main-chain scission, and the destruction of the crosslinked network.[31] In comparison with the decomposition procedure of the HPG/PAA hydrogel and that of the HPG hydrogel, the thermal stability of the HPG/PAA hydrogels increased apparently. This phenomenon was caused by the enhancement of the hydrogen-bond interaction with the introduction of AA.

### Hydrogel Morphology

To demonstrate the dependence of the hydrogel morphology on the mass ratio of HPG to AA used in polymerization, SEM micrographs for the internal structures of the HPG/PAA hydrogels and HPG hydrogel were taken and are shown in Figure 4. The HPG/PAA hydrogels showed porous structures compared to the HPG hydrogel; this illustrated the introduction of AA, which led to a porous network structure.[32] With increasing AA content in the hydrogel, the size and amount of pores increased significantly. This phenomenon was caused by the strong electrostatic repulsions among carboxylate anions during polymerization. As a result, the porous structure in the HPG/PAA hydrogels increased the area of contact with water and the dye molecules effectively and facilitated them to diffuse into the polymeric network and improve the adsorption capacities of the hydrogel. Therefore, the copolymerization of HPG and AA produced a hydrogel with a porous structure that was suitable for the removal.

### Effect of the PAA Content on the Swelling Ratio

The effect of the PAA content on the swelling ratio of the HPG/PAA hydrogels is shown in Figure 5. The swelling ratio of the HPG/PAA hydrogel increased significantly with PAA content, and the HA5 sample (AA 5 g) showed the maximum swelling ratio. Combined with the SEM micrographs, we concluded that the swelling ratio of the HPG/PAA hydrogels depended on the number of hydrophilic groups and the internal structure of the hydrogel. The increase in the PAA content led to an enhancement in the electrostatic repulsion between $-COO^-$; this expanded the network of the HPG/PAA hydrogels, and more pores enhanced the uptake of water during the swelling procedure compared with that of the less porous hydrogel.

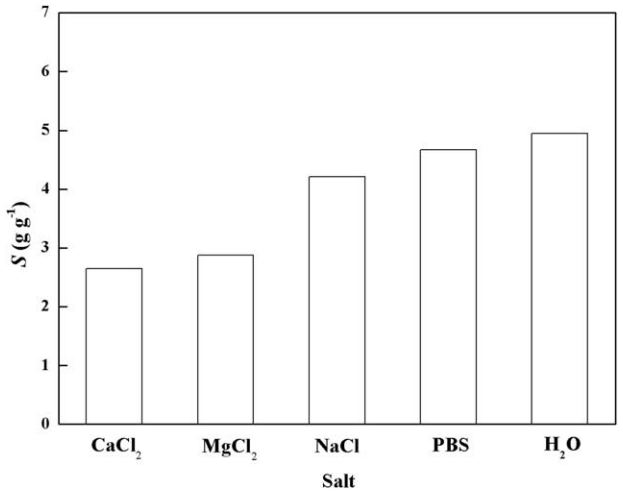


**Figure 8.** Effect of salt on the swelling ratio (PBS = phosphate buffer solution).

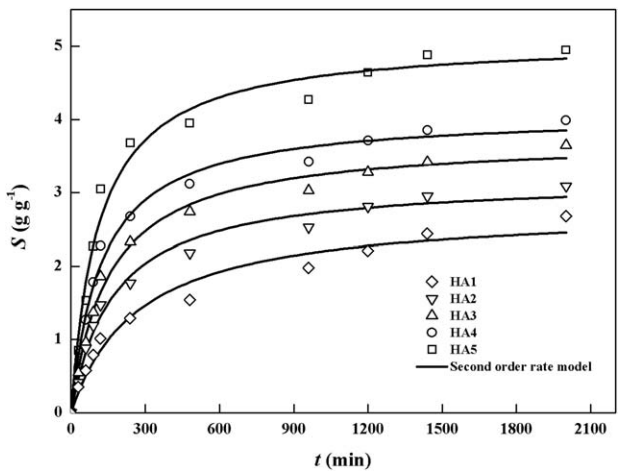


**Figure 9.** Fitting of the swelling data to a second-order rate equation.

**Table II.** Kinetics and Diffusion Parameters for the Swelling of the HPG/PAA Hydrogels

| Sample | $S_{eexp}$ (g/g) | $S_{ecal}$ (g/g) | $k_2$ (g $g^{-1}$ $min^{-1}$) | $R^2$ | $k_D$ ($s^{-1}$) | $m$ | $D \times 10^{10}$ ($m^2/s$) | $R^2$ |
|---|---|---|---|---|---|---|---|---|
| HA1 | 2.68 | 2.78 | 0.0013 | 0.9716 | 0.049 | 0.39 | 2.45 | 0.9901 |
| HA2 | 3.09 | 3.19 | 0.0018 | 0.9858 | 0.084 | 0.35 | 3.15 | 0.9706 |
| HA3 | 3.65 | 3.74 | 0.0017 | 0.9897 | 0.095 | 0.32 | 1.65 | 0.9531 |
| HA4 | 3.99 | 4.08 | 0.0019 | 0.9883 | 0.121 | 0.33 | 4.88 | 0.9431 |
| HA5 | 4.95 | 5.09 | 0.0176 | 0.9816 | 0.136 | 0.34 | 9.41 | 0.9217 |

### Temperature Dependence of the Swelling Ratio

Figure 6 illustrates the influence of the temperature on the swelling ratio of the HPG/PAA hydrogels. The swelling ratio of the HPG/PAA hydrogels increased significantly in the temperature range 15–50°C. Then, it remained stable in the temperature range 55–70°C. This phenomenon was caused by the interaction between carboxyl groups and hydroxyl groups in the hydrogels, as reported elsewhere.[33] The hydrogen bonds between the hydroxyl groups and carboxyl groups gradually ruptured with increasing temperature from 15 to 50°C. This led to a more expanded structure and a higher swelling ratio. In the temperature range 55–70°C, the swelling ratio changed a little, and this meant that the hydrogen-bond interactions were very weak in the hydrogels. This signified that the HPG/PAA hydrogels were more hydrophilic in the aqueous solution with high temperatures.

### pH Dependence of the Swelling Ratio

The pH sensitivity is an important property for hydrogels. The effluents discarded by factories are usually acidic or alkaline. So, it was necessary to investigate the influence of the pH value on the swelling ratio of the HPG/PAA hydrogels. The pH range of the medium was adjusted from 1 to 13, and the pH dependence for the swelling ratio of the HPG/PAA hydrogels was tested at 25°C. As shown in Figure 7, the swelling ratio of the HPG/PAA hydrogels increased with the pH value. This phenomenon was explained by the fact that with the neutralization of —COOH, the electrostatic repulsion of carboxyl anions was gradually enhanced, and this made the hydrogel more porous and hydrophilic.[34] The swelling ratio of the HPG/PAA hydrogels changed only a little (<1.5 times) in the pH range 1–11 compared with the previous PAA-based hydrogels (>4 times).[29,34] This showed that the HPG/PAA hydrogels remained relatively stable in the aqueous solution at a specific pH value. This phenomenon also signified that as the crosslinker, HPG enhanced the pH stability of the PAA-based hydrogel compared with the conventional crosslinker, *N*′,*N*-methylene bisacrylamide.[29,34]

### Effect of Salt on the Swelling Ratio

As far as we are concerned, the swelling behavior of a hydrogel is the final result of osmotic and restoring elastic pressures. The appearance of solute in an aqueous solution will tilt this balance and lead to changes in the swelling ratio. HA5 was chosen as a model sample because it had the highest AA content. As shown in Figure 8, HA5 showed swelling ratios of 2.65, 2.88, 4.21, 4.67, and 4.95 in five different solutions. In fact, the swelling of the hydrogels was caused by the electrostatic repulsion of the functional groups (e.g., —$COO^-$) when the hydrogel network was expanded by the easy penetration of water molecules. We observed that the swelling ratio of HA5 decreased apparently with the existence of monovalent ions ($Na^+$) and bivalent ions ($Mg^{2+}$ and $Ca^{2+}$). The metal ions, $Ca^{2+}$ and $Mg^{2+}$, could form intermolecular and intramolecular complexes with —$COO^-$ and —OH in the hydrogels, and this led to deswelling and contraction. The increased electrostatic attraction between the anionic sites of the chains and the multivalent cations also resulted in

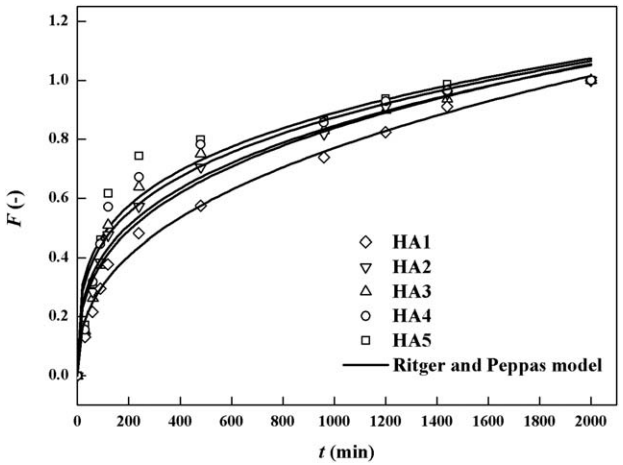


**Figure 10.** Fitting of the swelling data to the Ritger and Peppas model of diffusion.

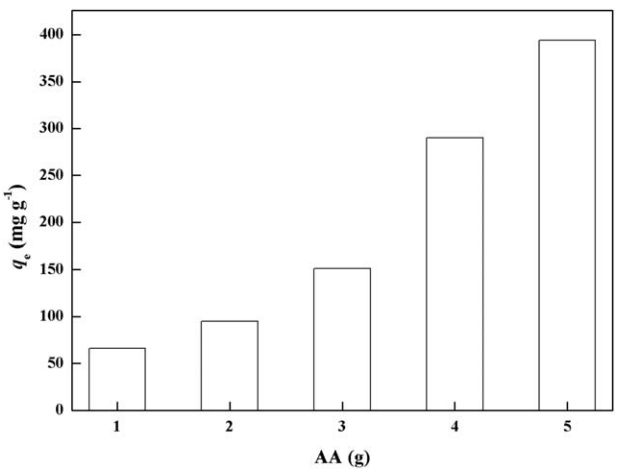


**Figure 11.** Effect of the PAA content on the dye adsorption.

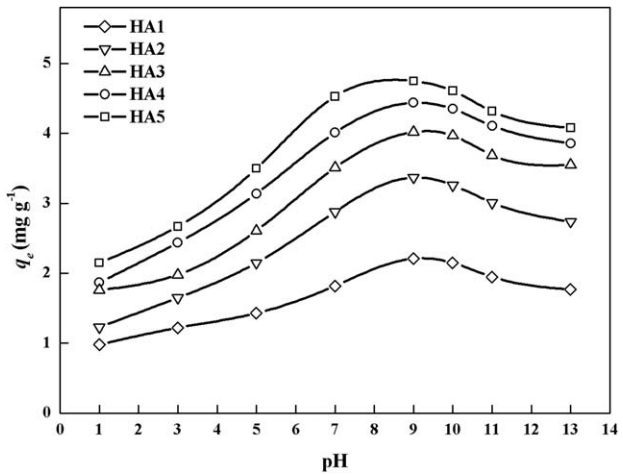


**Figure 12.** pH dependence of $q_e$ for the HPG/PAA hydrogels at a feed concentration of 5 mg/L.

an increase in the ionic crosslinking or the crosslinking density of the hydrogels, and this could lead to a rigid network and a loss of swelling.

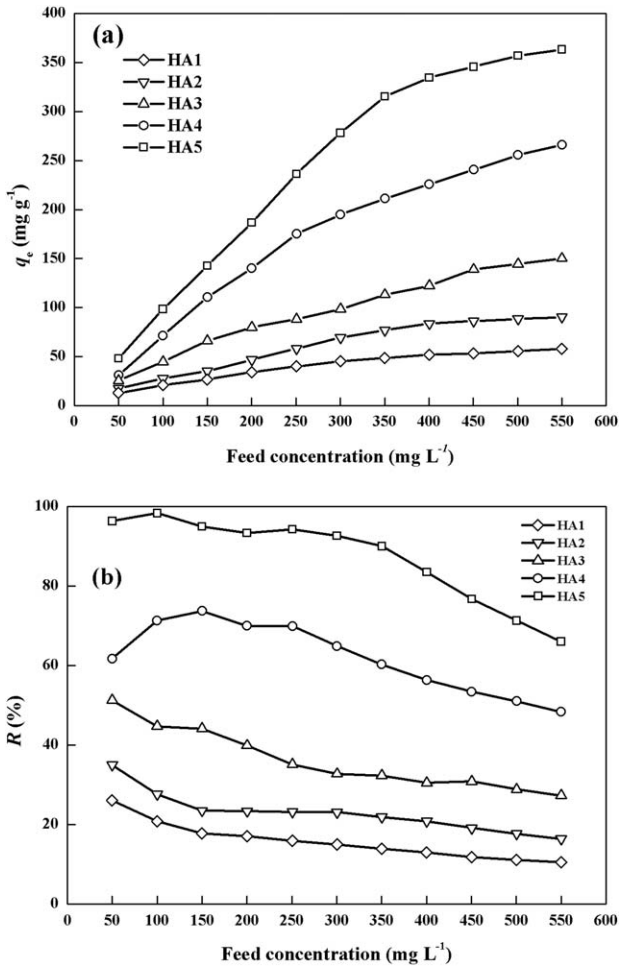


**Figure 13.** Effect of the feed concentration on the (a) $q_e$ and (b) removal ratio.

### Swelling Kinetics

The swelling data of the HPG/PAA hydrogels were directly fitted to the second-order rate equation and the results are shown in Figure 9 and Table II. As shown in Table II, $S_{ecal}$ was very close to the experimental equilibrium swelling ratio ($S_{eexp}$). The values of the correlation coefficient ($R^2$) were also observed to be greater than 0.95. All of these fittings clearly indicated close fitting of the swelling data of the HPG/PAA hydrogels to second-order rate kinetics.

### Diffusion Characteristics

In Figure 10, the fractional water uptake ($F$) are plotted against swelling time ($t$). The data were directly fitted to the equation of Ritger and Peppas to obtain the diffusion constant ($k_D$).[27] The diffusion coefficient ($D$) and diffusion exponent ($m$) of the HPG/PAA hydrogels were obtained from the following equations:

$$F=\frac{S_t}{S_e}=k_D t^m \tag{5}$$

$$D=\pi R^2\left(\frac{k_D}{4}\right)^{\frac{1}{m}} \tag{6}$$

where $S_e$ is the equilibrium swelling ratio. The values of $D$, $k_D$, $m$, and $R^2$ of the HPG/PAA hydrogels are also shown in Table II. The values of $R^2$ suggested a good fit with the nonlinear equation of Ritger and Peppas. In a subsequent study, the HPG/PAA hydrogels were used for the adsorption of MV in aqueous solutions with different feed concentrations.

### Effect of the PAA Content on the Dye Adsorption

The HPG/PAA hydrogels contained a large amount of carboxyl acid groups and hydroxyl groups, which were suitable for the removal of basic dyes. MV was chosen as a model compound to test the capacity of dye removal because it is a commonly carcinogenic organic pollutant in industrial wastewater. An MV solution with a concentration of 1 g/L was prepared, and 50 mg of hydrogel was added to a 50 mL MV solution to investigate the influence of the PAA content on $q_e$ at 25°C. As shown in Figure 11, the capacity of dye adsorption was enhanced significantly with increasing PAA content, and the sample HA5 showed the maximum $q_e$ of 394.12 mg/g. The high adsorption was caused by strong electrostatic interactions among the functional groups of the cationic dyes and anionic hydrogels. According to the previous analysis, HA5 possessed more carboxylic groups and a greater porous structure compared with HA1–HA4; this was beneficial for the adsorption and diffusion of dye molecules into the hydrogel.

### pH Dependence of the Dye Adsorption

The functional groups, such as carboxylic acid (from AA) and hydroxyl groups (from HPG), present in the HPG/PAA hydrogels changed with the pH of the aqueous solutions. Figure 12 also indicates that the swelling ratio of the HPG/PAA hydrogel changed with the pH value. Thus, the effect of the solution pH on $q_e$ was investigated in the MV solution of 5 mg/L. Figure 12 shows that $q_e$ was very low below pH 4 and that there was a significant increase in $q_e$ from pH 4 to 7. The low $q_e$ was due to the hydrogen bonds among the carboxylic, hydroxyl, and amine groups of the HPG/PAA hydrogels and the MV dye. The increase in $q_e$ was caused by the ionization of the carboxylate ions of PAA in the HPG/PAA hydrogels.[35] The decrease in $q_e$ above pH 9 was due to the

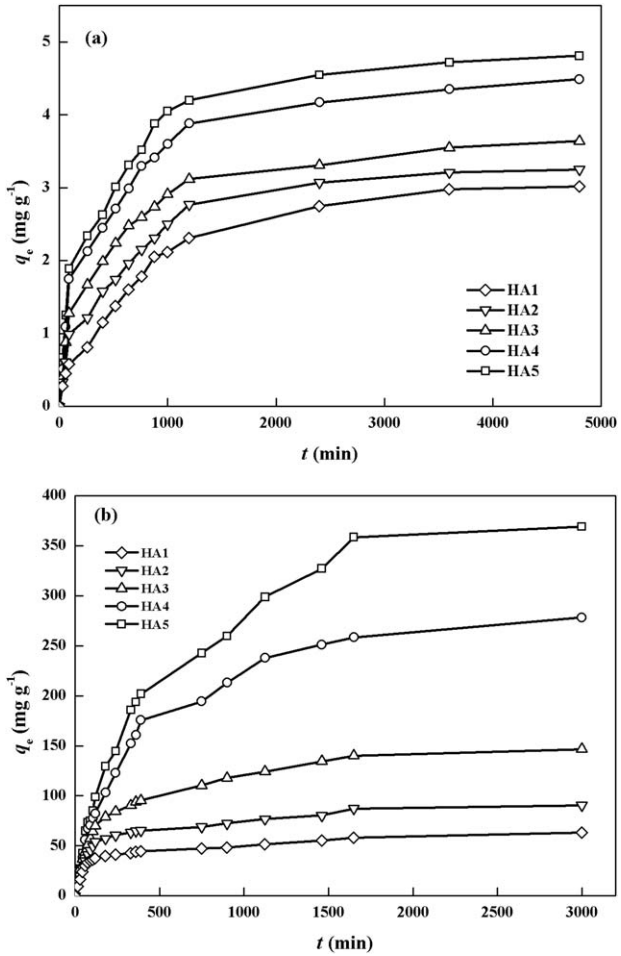


Figure 14. Effect of the contact time on the dye adsorption at a (a) low feed concentration of 5 mg/L and (b) high feed concentration of 1 g/L.

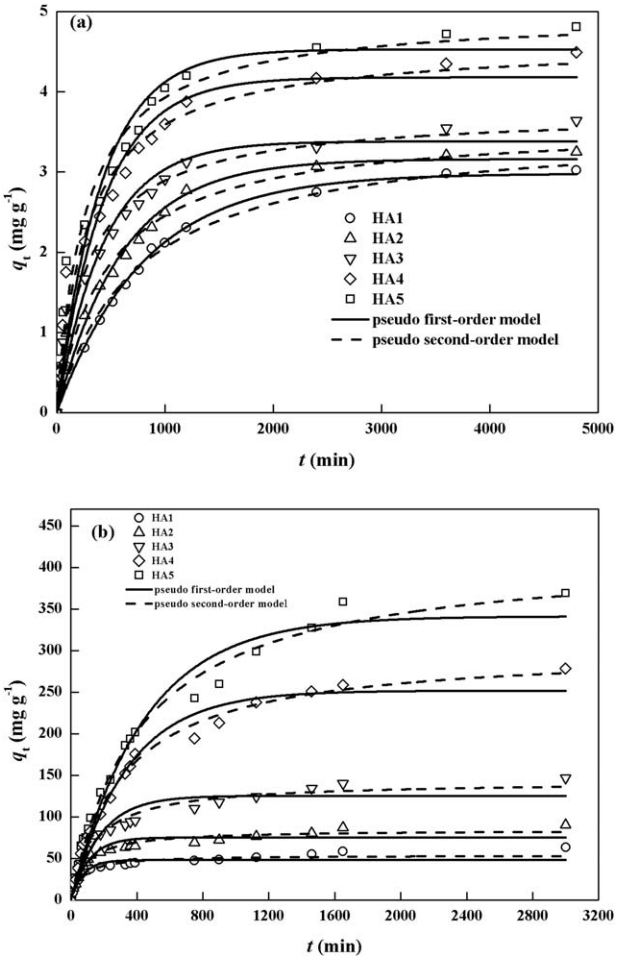


Figure 15. Effect of the contact time on the dye adsorption with fitting to the pseudo-first-order and pseudo-second-order models at a (a) low feed concentration of 5 mg/L and (b) high feed concentration of 1 g/L.

deprotonation of the amines groups of the MV dye. HA5 showed a higher maximum $q_e$ (4.75 mg) and a wider pH range (5–12) at high adsorption (> 4 mg/g) compared with the similar PAA-based hydrogel (maximum $q_e$ = 4.5 mg/g, pH range = 7–10) at a dye feed concentration of 5 mg/L.[27] This phenomenon further signified that HPG could enhance the pH stability of the PAA-based hydrogel and that the existence of terminal hydroxyl groups in HPG also contributed to dye adsorption.

Table III. Kinetic Parameters for the Adsorption of the MV Dye with the HPG/PAA Hydrogels

| | | Pseudo-first-order model | | | | Pseudo-second-order model | | |
|---|---|---|---|---|---|---|---|---|
| Concentration | Sample | Experimental $q_e$ (mg/g) | $k_1$ (min$^{-1}$) | Calculated $q_e$ (mg/g) | $R^2$ | $k_2$ (mg g$^{-1}$ min$^{-1}$) | Calculated $q_e$ (mg/g) | $R^2$ |
| 5 mg/L | HA1 | 3.02 | 0.0013 | 2.98 | 0.9864 | $3.84 \times 10^{-4}$ | 3.56 | 0.9874 |
| | HA2 | 3.25 | 0.0017 | 3.16 | 0.9644 | $5.96 \times 10^{-4}$ | 3.60 | 0.9778 |
| | HA3 | 3.64 | 0.0023 | 3.38 | 0.9462 | $8.95 \times 10^{-4}$ | 3.75 | 0.9795 |
| | HA4 | 4.49 | 0.0023 | 4.18 | 0.9335 | $7.63 \times 10^{-4}$ | 4.61 | 0.9708 |
| | HA5 | 4.81 | 0.0024 | 4.53 | 0.9333 | $7.55 \times 10^{-4}$ | 4.97 | 0.9698 |
| 1 g/L | HA1 | 66.09 | 0.0133 | 48.17 | 0.8361 | $2.95 \times 10^{-4}$ | 54.02 | 0.9126 |
| | HA2 | 94.79 | 0.0093 | 75.29 | 0.9308 | $1.36 \times 10^{-4}$ | 84.35 | 0.9745 |
| | HA3 | 150.93 | 0.0056 | 125.33 | 0.9288 | $4.73 \times 10^{-5}$ | 142.78 | 0.9794 |
| | HA4 | 289.87 | 0.0029 | 251.70 | 0.9772 | $1.03 \times 10^{-5}$ | 301.98 | 0.9937 |
| | HA5 | 394.12 | 0.0023 | 341.14 | 0.9739 | $5.64 \times 10^{-6}$ | 417.70 | 0.9902 |

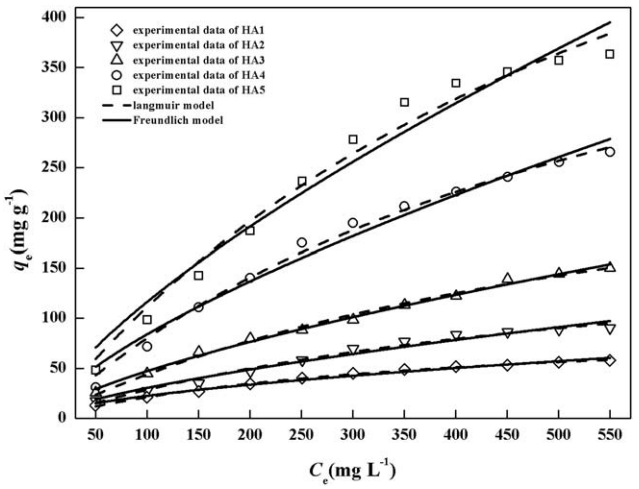


**Figure 16.** Effect of the feed concentration on $q_e$ with fitting to the Langmuir and Freundlich models.

### Effect of the Feed Concentration on the Dye Adsorption

Figure 13 shows the effect of the feed concentration on the $q_e$ and removal ratio of the HPG/PAA hydrogel at pH 7. With increasing PAA content, the $q_e$s and removal ratios of the HPG/PAA hydrogels increased significantly at both low and high feed concentrations. The sample of HA5 showed $q_e$s of 49.17 and 363.21 mg/g at feed concentrations of 50 and 550 mg/L, respectively. The corresponding removal ratios were 98.34 and 66.04%. MV is a cationic dye containing tertiary amine groups. Strong electrostatic interactions between the functional groups of the HPG/PAA hydrogels and dye molecules resulted in a high adsorption and removal ratio. The increase in the feed concentration led to an increase in $q_e$ when the removal ratio decreased because the adsorption capacity of a hydrogel is almost fixed and the amount of dye left in the solution is higher at a higher feed concentration.

### Effect of the Contact Time on the Dye Absorption

The effect of the contact time on the dye adsorption for both low (5 mg/L) and high (1 g/L) feed concentrations at pH 7 are shown in Figure 14. The dye adsorption increased rapidly; this was followed by a slower rate until it reached the equilibrium. At the beginning of adsorption, the functional groups of the HPG/PAA hydrogels were available for the interactions, and MV molecules quickly moved into the hydrogel network during the swelling process. Thus, the rate of dye adsorption was very high. When the functional groups were exhausted and the hydrogels gradually reached swelling equilibrium, the rate of dye adsorption decreased and finally reached dynamic equilibrium.[36] We observed that the equilibrium time for the feed concentration of 5 mg/L was longer than that of the feed concentration of 1 g/L. This phenomenon was caused by the reduction in the mass-transfer resistance for the transport of dye molecules at a high feed concentration, and thus, the equilibrium time was shorter than that at a low feed concentration.[37]

### Adsorption Kinetics

The pseudo-first-order equation of Lagergren and the pseudo-second-order equation of Ho and McKay were used to evaluate the kinetics of dye adsorption[27,35,38]:

$$q_t = q_e\left(1-e^{-k_1 t}\right) \tag{7}$$

$$q_t = \frac{q_e^2 k_2 t}{1+k_2 q_e t} \tag{8}$$

where $q_t$ is the adsorption at time $t$ (mg/g) and $k_1$ is the rate constant of the pseudo-first-order.

As shown in Figure 15 and Table III, the pseudo-second-model provided values of the calculated $q_e$ that were closer to most of the experimental ones than the pseudo-first-order model did, and $R^2$ of the pseudo-second-order model was larger than that of the pseudo-first-order model. Thus, the dye adsorption data fit the pseudo-second-order model better for both low and high feed concentrations; this signified that the electrostatic interactions among the functional groups of the hydrogels and MV dye determined the adsorption rate.[39]

### Adsorption Isotherms

The adsorption isotherms describe the relationship between the concentration of dissolved dyes in the liquid and the amount of dyes absorbed on the substrate at equilibrium. The Langmuir and Freundlich isotherms are commonly used to describe the adsorption characteristics of adsorbents used in water and wastewater.[27,35,38]

Langmuir:

$$q_e = \frac{q_m C_e b}{1+bC_e} \tag{9}$$

$$R_L = \frac{1}{1+bC_0} \tag{10}$$

Freundlich:

**Table IV.** Isotherm Parameters for the Adsorption of the MV Dye with the HPG/PAA Hydrogels

| | Freundlich model | | | Langmuir model | | | |
|---|---|---|---|---|---|---|---|
| | $k$ | $n$ | $R^2$ | $q_m$ (mg/g) | $b \times 10^3$ | $R^2$ | $R_L$ |
| HA1 | 1.55 | 1.72 | 0.9819 | 96.25 | 2.81 | 0.9954 | 0.392 |
| HA2 | 1.31 | 1.46 | 0.9714 | 194.86 | 1.73 | 0.9839 | 0.512 |
| HA3 | 1.94 | 1.44 | 0.9927 | 325.04 | 1.56 | 0.9928 | 0.538 |
| HA4 | 3.28 | 1.42 | 0.9767 | 572.50 | 1.63 | 0.9926 | 0.527 |
| HA5 | 4.28 | 1.39 | 0.9634 | 844.14 | 1.52 | 0.9818 | 0.544 |

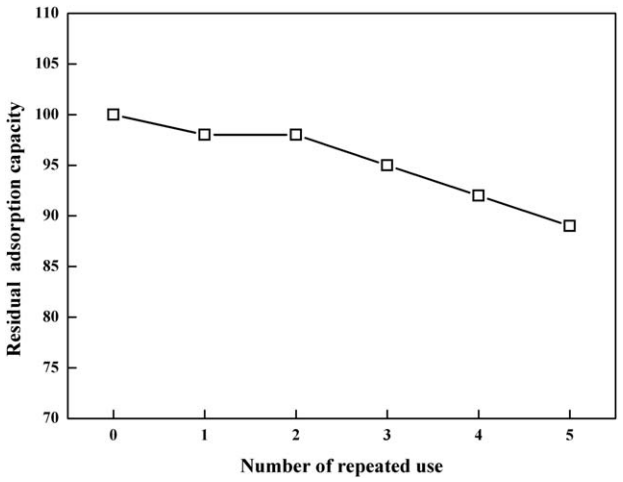


**Figure 17.** Reusability of the HPG/PAA hydrogel.

$$q_e = (kC_e)^{\frac{1}{n}} \quad (11)$$

where $q_m$ is the monolayer adsorption capacity (mg/g), $C_e$ is the dye concentration at equilibrium (mg/L), $b$ is the Langmuir constant ($cm^3$/g), $R_L$ is the separation factor of the Langmuir model, $C_0$ is the highest initial dye concentration (mg/L), and $k$ and $n$ are the Freundlich constants.

In the measurement experiments of the $q_e$ isotherms, 50 mg of the HPG/PAA hydrogel was immersed in 50-mL MV solutions with different concentrations (50–550 mg/L) to investigate the $q_e$ values of the HPG/PAA hydrogels. The adsorption isotherms of MV on the HPG/PAA hydrogels are displayed in Figure 16, and the fitting results are presented in Table IV. According to Table IV, the adsorption data fit the Langmuir model better than the Freundlich model. The $R_L$ values obtained from $C_0$ and $b$ for all of the HPG/PAA hydrogels were less than 1; this signified favorable adsorption.[40] Thus, we concluded that the adsorption of dye molecules occurred by monolayer formation on the hydrogel surface. The $q_m$ values increased with increasing PAA content; this illustrates that the cationic dye molecules were absorbed on the surface through direct bonding with carboxylic groups. When there were more active sites on the surface, the adsorption capacity was higher. This also agreed with the conclusion that an increase in the PAA content in hydrogels led to a high rate of dye adsorption. Overall, high amounts of carboxyl groups improved the dye adsorption rates and capacities of the hydrogels at the same time.

### Reusability of the HPG/PAA Hydrogels

The dye-loaded hydrogels were regenerated by desorption in a mixed solvent containing 0.1 mol/L hydrochloric acid and ethanol. As shown in Figure 17, the regenerated hydrogels were subjected to five repeated adsorption–desorption cycles where the adsorption capacity remained over 90%; this indicated the regeneration and reusability of the HPG/PAA hydrogels.

### Comparison of This Study with Other Reported Studies

The adsorption of MV dye by these HPG/PAA hydrogels is compared with other reported absorbents in Table V. From the results given in Table V, we observed that the dye adsorption by the hydrogels and other adsorbents were strongly influenced by the feed concentration. This hydrogel showed a higher adsorption than most of the reported hydrogels for both high and low feed concentrations.

**Table V.** Comparison of the Results of This Study with Reported Data

| Name of the hydrogel/other adsorbent | Dye concentration (mg/L) | Adsorption performance (mg/g) | Reference |
|---|---|---|---|
| Interpenetrating polymer network 2 | 2.5 | 1.723 | 36 |
| | 500 | 283.7 | |
| full-interpenetrating polymer network of chitosan and poly(methacrylic acid) | 500 | 221 | 41 |
| Semi-interpenetrating polymer network of sodium alginate and hydroxyethyl methacrylate | 100 | 90 | 42 |
| Poly(acrylamide co hydroxyethyl methacrylate) gel | 3 | 0.135 | 43 |
| Semi-interpenetrating of the starch and copolymer of acrylamide and hydroxyethyl methacrylate. | 250 | 156 | 44 |
| | 2.5 | 2.47 | |
| Soya ash | 25.9 | 4.209 | 45 |
| Chitosan/hexadecyl trimethyl ammonium bromide beads | 1000 | 373.29 | 46 |
| Duckweed | 600 | 332.5 | 47 |
| HA5 | 5 | 4.81 | This study |
| | 500 | 357.12 | This study |
| | 1000 | 394.12 | This study |

## CONCLUSIONS

In this study, hydrogels were synthesized from HPG and AA through free-radical polymerization. The characterizations of the HPG/PAA hydrogels by FTIR spectroscopy, TGA, and SEM showed that HPG acted as a monomer and crosslinker at the same time, and the presence of PAA chains in the hydrogels connected different HPG molecules to form a porous network structure. The swelling behaviors of the hydrogels investigated in different media showed that the HPG/PAA hydrogels were more hydrophilic in aqueous solution at higher temperatures

and they exhibited stability in a wide pH range of 1–11. The HPG/PAA hydrogels were further used for the adsorption of MV, and a maximum $q_e$ of 394.12 mg/g at a feed concentration of 1 g/L and a removal ratio of 98.33% at a feed concentration of 50 mg/L were observed. The dye adsorption data at different feed concentrations and time intervals fit well with the Langmuir isotherm and pseudo-second-order model. The HPG/PAA hydrogels exhibited the potential for applications in the removal of cationic dyes from aqueous solutions. In the meantime, the established biocompatibility of HPG and PAA suggested applications of this material in biomedical applications, such as enzyme immobilization and drug release.

## ACKNOWLEDGMENTS

The authors are grateful for the financial support of the National Natural Science Foundation of China (contract grant numbers 21073164).

## REFERENCES

1. Kayranli, B. *Chem. Eng. J.* **2011**, *173*, 782.
2. Walker, G. M.; Hansen, L.; Hanna, J. A.; Allen, S. J. *Water. Res.* **2003**, *37*, 2081.
3. Stydini, M.; Dimitris, I. K.; Verykios, X. E. *Appl. Catal. Environ.* **2004**, *47*, 189.
4. Kaustubha, M.; Naidu, J. H.; Meikap, B. C.; Biswas, M. N. *Ind. Eng. Chem. Res.* **2006**, *45*, 5156.
5. Misra, N.; Kumar, V.; Goel, N. K.; Varshney, L. *Polymer.* **2014**, *55*, 6017.
6. Singhal, R.; Singh, S. *J. Appl. Polym. Sci.* **2012**, *125*, 1267.
7. Hu, Z. G.; Zhang, J.; Chan, W. L.; Szeto, Y. S. *Polymer* **2006**, *47*, 5838.
8. Iyim, T. B.; Acar, I.; Ozgumus, S. *J. Appl. Polym. Sci.* **2008**, *109*, 2774.
9. Gong, R. M.; Ding, Y.; Li, M.; Yang, C.; Liu, H. J.; Sun, Y. Z. *Dyes Pigments* **2005**, *64*, 187.
10. Akkaya, M. C.; Emik, S.; Guclu, G.; Iyim, T. B.; Ozgumus, S. *J. Appl. Polym. Sci.* **2009**, *114*, 1150.
11. Maciejewski, M. *J. Macromol. Sci. Chem.* **1982**, *17*, 689.
12. Tomalia, D. A.; Naylor, A.; Goddard, W. A. *Angew. Chem. Int. Ed.* **1990**, *29*, 138.
13. Zeng, F.; Zimmerman, S. C. *Chem. Rev.* **1997**, *97*, 1681.
14. Wilm, D.; Stiriba, S. E.; Frey, H. *Acc. Chem. Res.* **2010**, *43*, 129.
15. Haag, R.; Sunder, A.; Stumbe, J. F. *J. Am. Chem. Soc.* **2000**, *122*, 2954.
16. Kramer, M.; Stumbe, J. F.; Turk, H.; Krause, S.; Komp, A.; Delineau, L.; Prokhorova, S.; Kautz, H.; Haag, R. *Angew. Chem. Int. Ed.* **2002**, *41*, 4252.
17. Kainthan, R. K.; Brooks, D. E. *Biomaterials* **2007**, *28*, 4779.
18. Roller, S.; Turk, H.; Stumbe, J. F.; Rapp, W.; Haag, R. *J. Comb. Chem.* **2006**, *8*, 350.
19. Zimmerman, S. C.; Quinn, J. R.; Burakowska, E.; Rainer, H. *Angew. Chem. Int. Ed.* **2007**, *119*, 8312.
20. Burakowska, E.; Quinn, J. R.; Zimmerman, S. C.; Rainer, H. *J. Am. Chem. Soc.* **2009**, *131*, 10574.
21. Zhou, L.; Gao, C.; Xu, W. J. *Appl. Mater. Interfaces* **2010**, *2*, 1483.
22. Sunder, A.; Hanselmann, R.; Frey, H.; Mulhaupt, R. *Macromolecules* **1999**, *32*, 4240.
23. Oudshoorn, M. H. M.; Rissmann, R.; Bouwstra, J. A.; Hennink, W. E. *Biomaterials* **2006**, *27*, 5471.
24. Zhou, Y. M.; Fu, S. Y.; Zhang, L. L.; Zhan, H. Y. *Carbohydr. Polym.* **2013**, *97*, 429.
25. Jin, S. P.; Liu, M. Z.; Zhang, F.; Chen, S. L.; Niu, A. Z. *Polymer* **2006**, *47*, 1526.
26. Pourjavadi, A.; Jahromi, P. E.; Seidi, F.; Salimi, H. *Carbohydr. Polym.* **2010**, *79*, 933.
27. Bhattacharyya, R.; Ray, S. K. *Chem. Eng. J.* **2015**, *260*, 269.
28. Chen, Z. J.; Zhou, L.; Zhang, F.; Yu, C. B.; Wei, Z. B. *Appl. Surf. Sci.* **2012**, *258*, 5291.
29. Zhao, Y.; Kang, J.; Tan, T. W. *Polymer* **2006**, *47*, 7702.
30. Wang, S. X.; Zhou, Y.; Yang, S. C.; Ding, B. J. *Colloid Surf. B* **2008**, *67*, 122.
31. Mandal, B.; Ray, S. K. *Mater. Sci. Eng. C* **2014**, *44*, 132.
32. Zhang, G. Q.; Zha, L. S.; Zhou, M. H.; Ma, J. H.; Liang, B. R. *J. Appl. Polym. Sci.* **2005**, *97*, 1931.
33. Kim, B.; Hong, D.; Chang, W. V. *J. Appl. Polym. Sci.* **2013**, *130*, 3574.
34. Mahdavinia, G. R.; Pourjavadi, A.; Hosseinzadeh, H.; Zohuriaan, M. J. *Eur. Polym. J.* **2004**, *40*, 1399.
35. Ray, S. K.; Maity, J. *Carbohydr. Polym.* **2013**, *217*, 192.
36. Bhattacharyya, R.; Ray, S. K. *J. Polym. Eng. Sci.* **2013**, *11*, 2439.
37. Bayramoglu, G.; Altintas, B.; Yakup, A. M. *Chem. Eng. J.* **2009**, *152*, 339.
38. Wu, J. S.; Liu, C. H.; Chu, K. H.; Suen, S. Y. *J. Membr. Sci.* **2008**, *309*, 239.
39. Ghouti, M. A.; Khraisheh, M.; Ahmad, S. A. *J. Colloid Interface Sci.* **2005**, *287*, 6.
40. Baskaralingam, P.; Pulikesi, M.; Elango, D.; Ramamurthi, V.; Sivanesan, S. *J. Hazard. Mater.* **2006**, *128*, 138.
41. Maity, J.; Ray, S. K. *Carbohydr. Polym.* **2014**, *104*, 8.
42. Mandal, B.; Ray, S. K. *Carbohydr. Polym.* **2013**, *98*, 257.
43. Bhattacharyya, R.; Ray, S. K.; Mandal, B. *J. Ind. Eng. Chem.* **2013**, *19*, 1191.
44. Bhattacharyya, R.; Ray, S. K. *J. Ind. Eng. Chem.* **2014**, *20*, 3714.
45. Gupta, V. K.; Mittal, A.; Gajbe, V. *J. Colloid Interface Sci.* **2008**, *319*, 30.
46. Chatterjee, S.; Lee, M. W.; Woo, S. H. *Chem. Eng. J.* **2009**, *155*, 254.
47. Lim, L. B. L.; Priyantha, N.; Chan, C. M.; Matassan, D.; Chieng, H. I.; Kooh, M. R. R. *Arab. J. Sci. Eng.* **2014**, *39*, 6757.